

## Electron Vortex Dynamics in an Applied Shear Flow

D.L. Eggleston

*Occidental College, Department of Physics  
Los Angeles, California 90041*

**Abstract.** An electron column in a modified Malmberg-Penning trap is used to study the behavior of a single two-dimensional vortex in an imposed irrotational shear flow. Phosphor screen images of the shearing process show a variety of phenomena including the fission of the original vortex, the emission, stretching, and entrainment of filamentary arms, and turbulent diffusion. The vortex lifetime is measured as a function of applied shear, with vortex strength independently adjustable. These data are compared to the predictions of a fluid theory which correctly identifies the key dimensionless parameter (shear rate/vorticity) but not its critical value.

### Introduction

A basic issue in vortex dynamics concerns the fate of a two-dimensional (2-D) vortex in a shear flow (plane strain). The interaction can be described as a competition between the shearing flow, which tries to disperse the vortex, and the vortical motion, which tries to maintain the vortex. Moore and Saffman<sup>1</sup> studied this problem analytically and found that an elliptical vortex patch (i.e. a region of constant vorticity bounded by an ellipse) could exist in an irrotational shear flow only if the strain rate was less than a critical value. Kida<sup>2</sup> later showed that when the strain rate exceeded this value the ellipse would undergo irreversible elongation and thus the vortex would be dispersed.

The work of Moore & Saffman and Kida is based on the classical theory of inviscid, constant density fluids as modeled by the Euler equations. As noted recently by Driscoll and Fine<sup>3</sup>, such work can be applied directly to strongly magnetized pure electron plasmas since the two-dimensional drift-Poisson equations describing such plasmas are isomorphic to the Euler equations. In the plasma system the vorticity (a key fluid quantity) is proportional to the electron density, and is thus easily measured, while the viscosity and boundary drag are very small. These

features make such systems ideal for testing 2-D vortex theory.

In this paper an electron column system is used to study the behavior of a single 2-D vortex in an imposed irrotational shear flow. The vortex evolution in a strong shear is characterized by the emission of filamentary arms and sometimes by the fission of the original vortex. The vortex lifetime is measured as a function of applied shear, with vortex strength independently adjustable, and compared to the prediction of Moore & Saffman. Consistent with their theory, the vortex lifetime increases significantly when the applied shear is less than a critical value. For subcritical shear values the vortex lifetime appears to be limited by a slow diffusion which gradually weakens the vortex.

### Experimental Device

The apparatus used in these experiments, shown schematically in Fig. 1a, is a modified Malmberg-Penning trap. A long conducting cylinder is divided axially into eight electrically isolated parts labelled G1, S1, S2, S3, S4, S5, G2, and G3. Each of these cylinders is 6.00" long, has an I.D. of 3.05", and is separated from the others by a gap of 0.050". Two of the cylinders (G1 and G2) act as gates for the trap while the others are normally grounded and provide a well-defined boundary condition for the trapped electrons. Each of the cylinders S1 through S5 is divided azimuthally into eight sections which can be used to monitor the azimuthal motion of the electrons. The apparatus is placed in a vacuum of  $< 10^{-9}$  Torr and is immersed in a uniform axial magnetic field produced by a large solenoid. For these experiments  $B = 500$  G. At this magnetic field strength the Larmor radius is less than 0.1 mm and the electron dynamics are well described by the  $E \times B$  drift motion.

The above description is fairly common for Malmberg-Penning traps. Some distinctive features of this apparatus are as follows: The electrons are produced by a small diameter (0.1") oxide-coated cathode which is placed off-axis ( $r = 1.55$  cm.). This is used to inject a column of electrons into the system. The column's self-field causes it to spin around its axis (i.e., it forms a vortex). A long, thin (0.014" diam.), conducting wire which can be biased by the operator runs along the axis of the device. This is used to produce a radial electric field, and thus an azimuthal  $E \times B$  drift velocity, which is a function of radius and has zero curl (i.e., an irrotational shear

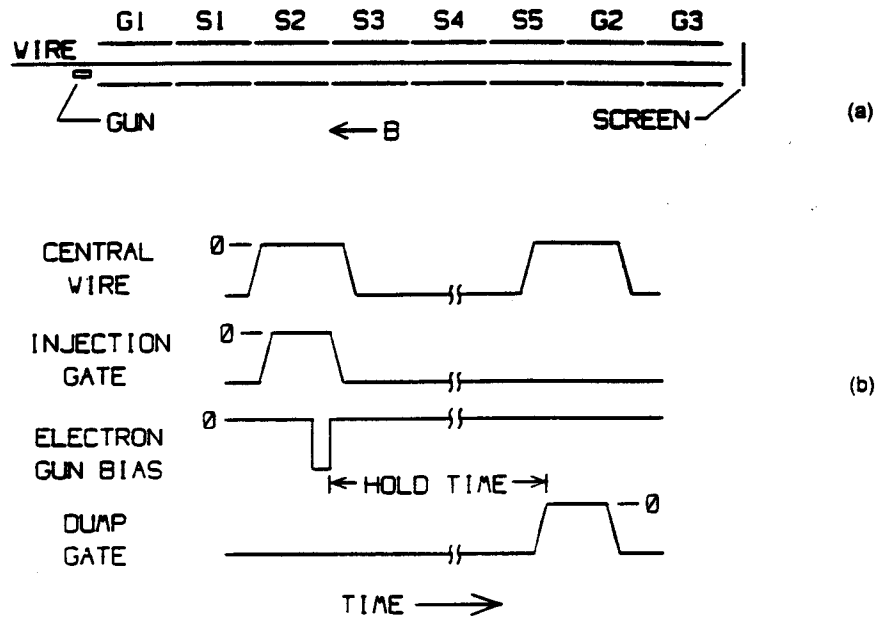


**FIGURE 1.** a) Schematic of experimental apparatus and b) timing diagram for one cycle of the experiment. Voltages applied to the central wire, injection gate (G1), electron gun, and dump gate (G2) are shown.

flow). The voltage  $\phi_{cw}$  placed on the central wire of the device can be either negative or positive, and thus the applied shear flow can either oppose the vortex rotation (adverse shear) or favor it (favorable or prograde shear). Finally, a phosphor-coated screen is used to measure the total charge of the dumped electrons and to produce an image that shows the position and density of the electrons. The images are acquired with a CCD camera and stored and analyzed with a computer-controlled frame grabber.

The apparatus is run in cycles as shown in Fig. 1b. To start a cycle, the central wire bias and injection gate bias are switched to zero and a negative pulse is applied to the electron gun. This allows an off-axis column of electrons to fill the device. The density of the electrons can be adjusted by changing the gun bias. The injection gate is then returned to a negative bias which traps the electrons between G1 and G2. The central wire bias is then switched to a selected value, thus producing a shear flow. After a time selected by the operator, the central wire and the gate G2 are grounded, allowing the electrons to stream out of the device along magnetic field lines and be collected by the positively biased phosphor screen. The total charge in the machine at the time of the dump is thus obtained, as well as an axially integrated image of the electron positions. Typically, several cycles are

required to produce enough light for a visible image. On subsequent cycles the hold time can be varied, so that a sequence of images representing the time evolution of the vortex is produced. The shot-to-shot variation in the injected vortex is small enough that each shot evolves identically for 20-80  $\mu$ s after which shot-to-shot variations in the dump-time position of the vortex cause a smearing of the multi-cycle image. After this point one or more of the azimuthal sectors of cylinders S1 - S5 can be used to monitor the azimuthal motion of the vortex. This is done by attaching the sector to ground through a resistor and observing the voltage fluctuations across the resistor produced by the variations in the vortex image charges. Since only the amplitude of these signals is of interest, the shot-to-shot phase differences can be ignored.

### Theoretical Model

The important quantities in the theoretical model of Moore & Saffman/Kida are the vorticity of the elliptical patch  $\Omega$  and the strain rate  $e$ . The vorticity, which we define to be positive for our electron column, is given by  $\Omega = nq/\epsilon_0 B$  where  $n$  is the electron density,  $q$  is the electron charge and  $B$  is the magnetic field strength. The theory assumes the vorticity is constant within the boundaries of the patch, whereas the density profile of our vortices is roughly Gaussian. To compare with theory, we assume that our vortex is comparable to a circular patch of radius  $R_v$  and density  $N_L/\pi R_v^2$ . Here  $N_L = \int n dA/L$  is the number of electrons per unit length,  $L$  is the length of the column,  $R_v = 1.5 \int n |r - R_{cm}| dA / N_L$ ,  $R_{cm} = \int n r dA / N_L$  is the position of the vortex center of mass,  $n = n(r, \theta)$  is the density which is determined from the pixel value at  $r = (r, \theta)$ , and the integral is over the cross sectional area of the device. The strain rate (or maximum rate of extension)  $e$  is defined in a frame where the vortex center is at rest. For our case, this will be a frame rotating with angular velocity  $\omega(R_{cm})$ , where  $\omega(r) = v(r)/r$  and  $v$  is the  $E \times B$  drift velocity produced by the biased center wire (plus a small component due to the vortex image charges). In this frame the applied flow is simple shear and  $e = r(d\omega/dr)/2$  evaluated at  $r = R_{cm}$ . The strain rate is positive for positive center wire bias (i.e., the favorable shear case for the electron vortex). With these definitions, the key theoretical prediction can be simply stated: vortices with  $e/\Omega < -(3-2\sqrt{2})/2 \approx -0.086$  will be dispersed, those with  $e/\Omega > -0.086$  will

remain. The theory assumes that in either case the vortex will remain an elliptical patch, although the axis ratio and orientation may change.

In order to make a valid comparison with theory, the system parameters should be adjusted to satisfy the 2-D approximation. This requires that the axial transit time of the electrons be small compared to the time for motions in the  $r-\theta$  plane. Two characteristic  $r-\theta$  motions are the vortex spin around its own axis and its drift around the machine axis. Let  $\gamma_s$  denote the axial transit time over the vortex spin time and  $\gamma_d$  the transit time over the drift time. For the parameters of these experiments  $\gamma_s = 0.08 - 0.4$  and  $\gamma_d = 0.003 - 0.25$  so the 2-D approximation is reasonable. End effects which can break the 2-D assumption are also negligible.

Finally, we note that the theory approximates the applied strain by employing a linear Taylor expansion around the center of the vortex. The next term in the expansion goes like  $2R_v/R_{cm}$ . In our experiments  $2R_v/R_{cm} = 0.25$  so the expansion is reasonable.

### Qualitative Behavior of a Dispersing Vortex

Examples of vortex evolution are shown in the phosphor screen images of Figs. 2-4. Except as noted, the screen bias is adjusted for each image so that full exposure is obtained; if this were not done the later images would be too dim to distinguish details. Also, we display negative images: darker parts of the image correspond to brighter parts of the phosphor screen and higher electron densities.

Fig. 2a shows the initial vortex. For this case  $R_{cm} = 1.55$  cm and  $R_v = 1.9$  mm. The calculated density  $n$  is  $2.08 \times 10^7$  cm $^{-3}$ ,  $\phi_{cw} = -78.1$ V, and  $e/\Omega = -0.16$ . The vortex center drifts clockwise around the central wire. As shown in Figs. 2b and 2c, the vortex begins to disperse by emitting filamentary arms (these two images are overexposed so that these low density arms are visible). As time goes on, the arms continue to grow longer and wrap around the central wire (Figs. 2d-f). (Note: the vertical shadow in the images is produced by a bar which supports the central wire). The filaments wind into a tighter and tighter spiral until the detail can no longer be resolved (Fig. 2g).

Figure 3 shows the evolution for a slightly smaller shear ( $n = 2.08 \times 10^7$  cm $^{-3}$ ,  $\phi_{cw} = -69.5$ V,  $e/\Omega = -0.14$ ). The initial evolution is similar (Fig. 3a), but as the inner filamentary arm completes its first wrap around the central wire it re-joins the vortex (Fig. 3b; again Figs. 3a-c are overexposed to show detail). The

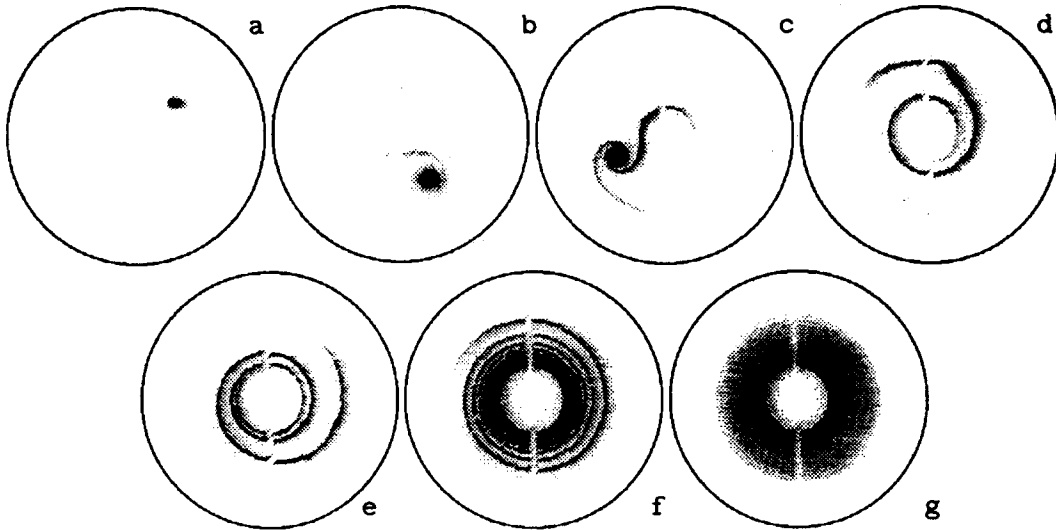


FIGURE 2. Phosphor screen images showing the emission of filamentary arms. Here  $e/\Omega = -0.16$ . Left to right,  $t(\mu s) = 0, 1.40, 2.70, 5.92, 9.02, 30.0$ , and  $110$ .

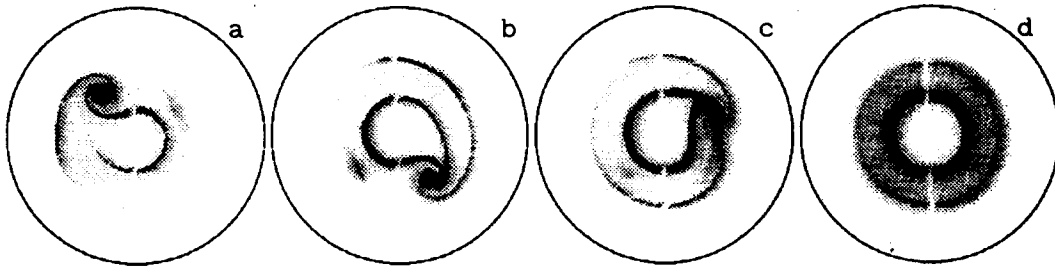
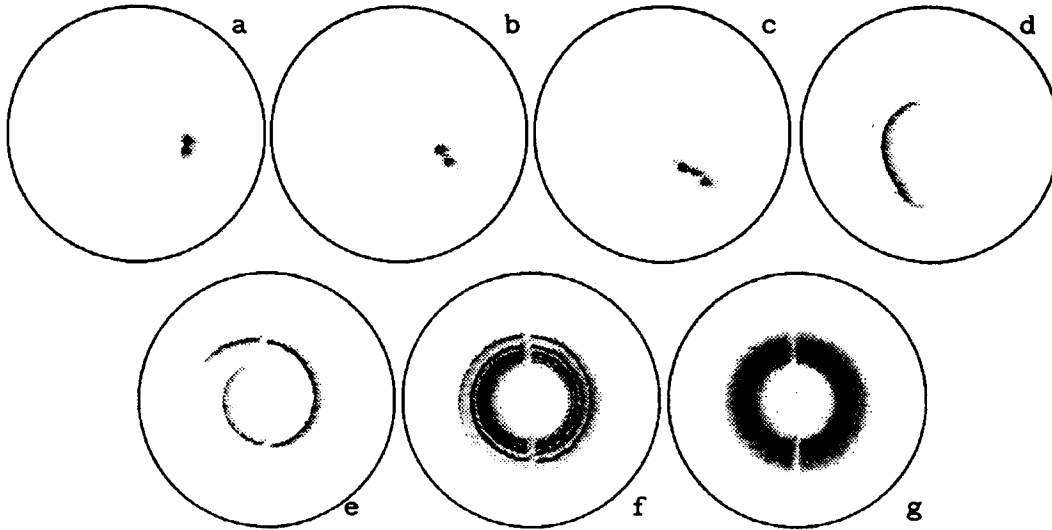


FIGURE 3. Phosphor screen images showing the entrainment of filamentary arm. Here  $e/\Omega = -0.14$  and  $t(\mu s) = 4.76, 8.06, 20.1$ , and  $135$ .

subsequent evolution shows turbulent variation from shot to shot; Fig. 3c is an average of eight shots. The turbulent dispersal of the vortex finally leads to a reproducible end state (Fig. 3d). Note that this end state is qualitatively different than the previous case (cf. Fig. 2g).

A final example of vortex evolution is shown in Fig. 4. Here the shear is stronger than in Fig. 2 and the density is lower:  $n = 9.33 \times 10^6 \text{ cm}^{-3}$ ,  $\phi_{cw} = -138.8 \text{ V}$ ,  $e/\Omega = -0.64$ . Rather than emitting filamentary arms the initial vortex undergoes fission, splitting into two and then three smaller vortices before being smeared into a long filament. The winding process then proceeds as before. The end state exhibits a more uniform distribution of electrons than the previous



**FIGURE 4.** Phosphor screen images showing the breakup (fission) of initial vortex. Vortex at  $t = 0$  looks the same as in Figure 2a. Here  $e/\Omega = -0.64$  and  $t(\mu s) = 0.58, 0.68, 0.90, 1.70, 3.40, 13.6,$  and  $77.0$ .

cases. In general, this vortex fission occurs when  $e/\Omega$  is large and negative (i.e. large adverse shear and low electron density).

#### Measurements of Vortex Lifetime

In order to quantify the shearing process it is useful to define a quantity  $T_s$ , which measures the time it takes to shear (i.e., disperse) the vortex. The definition of  $T_s$  is chosen so that the two methods available for monitoring the vortex dynamics (i.e., screen images and wall probe signals) give comparable values. For images, the electron center of mass  $R_{cm}$  is calculated. Since the sector probe measures electrons within its  $45^\circ$  angular span, all pixel values within the span  $\theta_{cm} \pm 22.5^\circ$  are summed and divided by the sum at  $t = 0$  (here  $\theta_{cm}$  is the angle of the vector  $R_{cm}$ ). The shear time  $T_s$  is defined as the time when this ratio drops to 0.5 (i.e. when half of the electrons have left the octant defined by  $\theta_{cm} \pm 22.5^\circ$ ). When the sector probe is used  $T_s$  is defined as the time when the amplitude of the probe signal drops to half of its initial value.

Data showing  $T_s$  versus the central wire bias  $\phi_{cw}$  with column density (vorticity) as a parameter are presented in Fig. 5. The solid symbols are data points taken from screen images and the open symbols are data points acquired with the wall probe. The qualitative

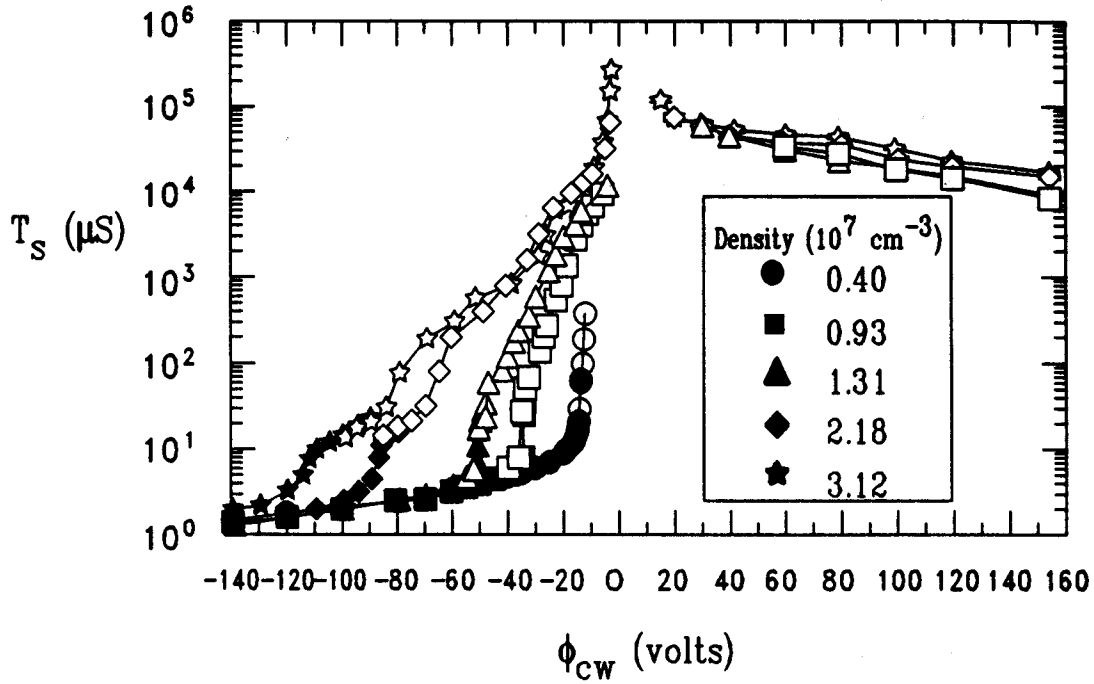


FIGURE 5. Vortex shear time  $T_s$  versus central wire bias  $\phi_{cw}$  with column density as a parameter.

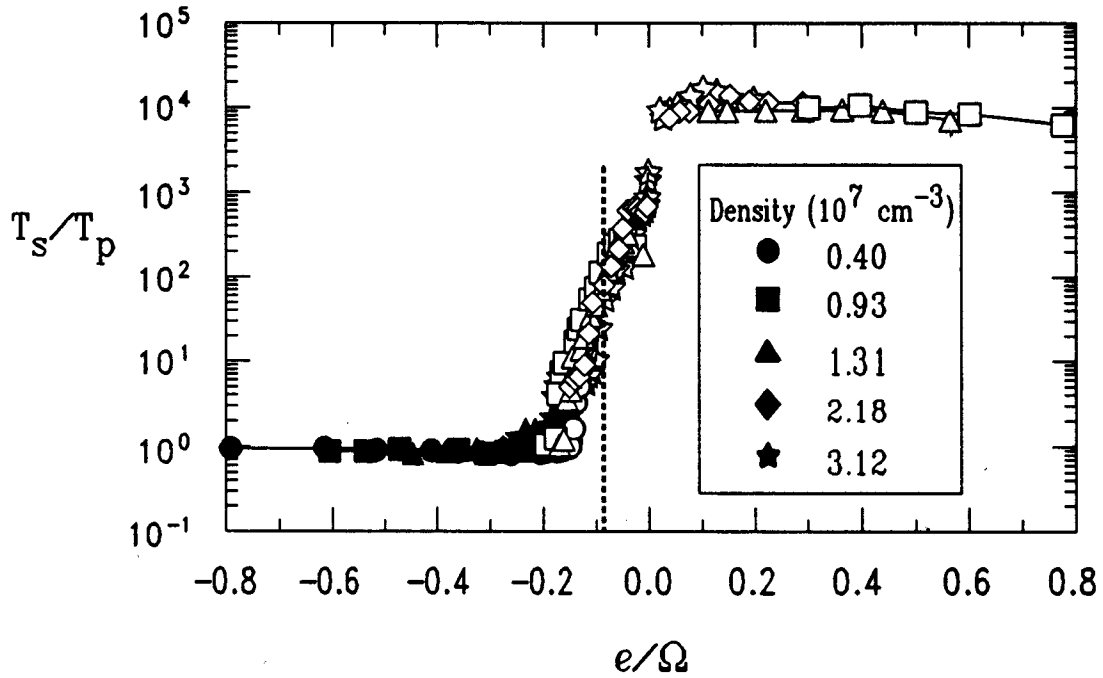


FIGURE 6. Data of Fig. 5 plotted using the normalizations suggested by theory. Dashed vertical line shows the theoretical critical value.



features are consistent with expectations. When the shear is adverse and large (large negative values of  $\phi_{cw}$ ), the vortex is quickly dispersed (small  $T_s$ ). As the shear is reduced ( $\phi_{cw}$  is made less negative), the vortex lifetime increases. The shear value at which this increase occurs depends on the column's density (vorticity); more shear is required to disperse a stronger vortex. We also note that for favorable shear ( $\phi_{cw} > 0$ ) the vortex lifetime is long and roughly independent of the value of  $\phi_{cw}$ .

In Fig. 6 this data is replotted using scaled quantities. The shear time  $T_s$  has been scaled to the passive shear time  $T_p$ , which is the time it would take to shear a column with zero vorticity. We take this time to be  $R_{cm}\theta_s/2eR_v$  where  $\theta_s$  is the angular spread defining vortex dispersal (here taken as  $\pi/4$  rad). On the abscissa is plotted the shear strength  $e$  divided by the vorticity  $\Omega$ , as suggested by theory.

The data now form one curve, showing that the scalings employed are the correct ones. The lifetime of a dispersing vortex is essentially  $T_p$ , and the parameter that determines the fate of the vortex is  $e/\Omega$ . When  $e/\Omega$  exceeds a critical value, the scaled vortex lifetime increases suddenly. The experimental critical value is slightly different for each of the cases considered, but the values do not exhibit any systematic dependence on density. The average experimental value is  $(e/\Omega)_{crit} = -0.163 \pm 0.015$ , in contrast with the theoretical value of  $-0.086$ . The vortex lifetime does not increase indefinitely at  $(e/\Omega)_{crit}$ . Rather, the lifetime jumps up abruptly by an order of magnitude and then follows a roughly exponential dependence on  $e/\Omega$ , reaching a roughly constant maximum value of  $10^4 T_p$  for  $e/\Omega > 0$ .

The dependence of  $T_s/T_p$  on  $e/\Omega$  for  $e/\Omega > (e/\Omega)_{crit}$  can be explained as follows. The wall probe signal is qualitatively different for  $(e/\Omega)_{crit} < e/\Omega < 0$  and  $e/\Omega > 0$ . For the first case, the signal is roughly constant in time and then decreases abruptly, signaling that the vortex has been dispersed. Limited phosphor screen imaging corroborates this interpretation of the wall probe signal. For  $e/\Omega > 0$ , the probe signal decreases gradually until it is lost in the noise. The imaging data for this case shows that the vortex remains unsheared and that  $R_{cm}$  remains roughly constant. Both cases may be explained by the presence of a slow diffusive transport. When  $(e/\Omega)_{crit} < e/\Omega < 0$  this transport causes the vortex density (and thus  $\Omega$ ) to decrease until  $e/\Omega$  falls below  $(e/\Omega)_{crit}$ , at which point the vortex will be dispersed. For  $e/\Omega > 0$ , the shear is unable to disperse the vortex irregardless of the value of  $\Omega$ , so the probe signal slowly decreases as

electrons diffuse. The nature of this diffusion is unknown, but it is significantly faster than the transport that leads to particle loss. The time to lose half the electrons from the device is roughly ten seconds, whereas the maximum vortex lifetimes are on the order of 0.1 s.

We can offer no explanation for the factor-of-two discrepancy between experimental and theoretical values for the critical  $e/\Omega$ . One can identify several areas where the experiment departs from the theoretical model (e.g., Gaussian vortex profile) but a quantitative analysis of such effects is, to our knowledge, not available.

### Conclusions

A vortex in a strong shear exhibits a variety of behaviors: vortex fission, filament emission, stretching, and entrainment, and turbulent diffusion. While none of these behaviors is included in the theory of Moore & Saffman/Kida, their theory correctly identifies the key dimensionless parameter  $e/\Omega$ . However, the predicted critical value is roughly half of the experimental value. When  $e/\Omega$  is less than the critical value the vortex lifetime is the same as that of a zero vorticity patch. When  $e/\Omega$  is above the critical value the vortex lifetime increases dramatically and appears to be limited by a slow diffusive process that gradually weakens the vortex.

### Acknowledgments

The author gratefully acknowledges Dr. C.F. Driscoll's advice on the design of Malmberg-Penning traps; seminal discussions of vortex dynamics with Dr. K.S. Fine; and Dr. Pei Huang for pointing out an important error in the original manuscript. This work was supported by ONR grant N00014-89-J-1399.

### References

1. D.W. Moore and P.G. Saffman, in Aircraft Wake Turbulence, edited by J. Olsen, A. Goldberg, and N. Rogers, (Plenum, New York, 1971), pp. 339-354.
2. S. Kida, J. Phys. Soc. Jpn. 50, 3517 (1981).
3. C.F. Driscoll and K.S. Fine, Phys. Fluids B 2, 1359 (1990).